Superionicity and Polymorphism in Calcium Fluoride at High Pressure

Claudio Cazorla[1,*] and Daniel Errandonea[2]
[1]School of Materials Science and Engineering, University of New South Wales, Sydney, New South Wales 2052, Australia
[2]Departamento de Física Aplicada (ICMUV), Universitat de Valencia, 46100 Burjassot, Spain
(Received 23 May 2014; revised manuscript received 18 September 2014; published 4 December 2014)

We present a combined experimental and computational first-principles study of the superionic and structural properties of CaF_2 at high $P-T$ conditions. We observe an anomalous superionic behavior in the low-P fluorite phase that consists of a decrease of the normal → superionic critical temperature with compression. This unexpected effect can be explained in terms of a P-induced softening of a zone-boundary X phonon that involves exclusively fluorine displacements. Also we find that superionic conductivity is absent in the high-P cotunnite phase. Instead, superionicity develops in a new low-symmetry high-T phase that we identify as monoclinic (space group $P2_1/c$). We discuss the possibility of observing these intriguing phenomena in related isomorphic materials.

DOI: 10.1103/PhysRevLett.113.235902 PACS numbers: 66.30.H−, 45.10.−b, 62.50.−p, 81.30.Dz

Alkali earth metal fluorides (i.e., AF_2 compounds with $A = $ Ca, Sr, and Ba) blend a family of extraordinary materials that for more than six decades have seduced both fundamental and applied physicists. Because of their low refractive index, low dispersion, and large broadband radiation transmittance, AF_2 compounds have been extensively employed in optical devices [1,2]. These are also promising candidates for solid-state electrolytes to be used in batteries, as their internal electric currents dwell on the motion of ions [3–7]. CaF_2 is an archetypal ionic conductor and the most representative of AF_2 species. Under ambient conditions CaF_2 crystallizes in the fluorite structure (α, space group $Fm\bar{3}m$) wherein Ca atoms are cubic coordinated to F atoms. In α-CaF_2 a strong increase of the ionic conductivity is observed as T is raised up to ∼1400 K [8–10]. At this point the mobility of the fluorine anions is comparable to that of a molten salt, while the melting temperature of the system lies ∼300 K higher [11,12].

The accepted dominant effect behind the large ionic conductivity observed in α-CaF_2, dubbed "superionicity," is the formation of point Frenkel pair defects (FPD) (i.e., simultaneous creation of F^- vacancies and interstitials) [4,5]. Yet, superionicity requires abundant and correlated anion displacements; therefore, the formation of FPD itself appears to be insufficient to fully elucidate the atomic mechanisms underlying it [13–15]. Moreover, this singular transport phenomenon remains surprisingly unexplored at moderate and high compressions. Almost 40 years ago, Mirwald and Kennedy were the first (and to the best of our knowledge the only ones so far) to experimentally study the high $P-T$ phase diagram of CaF_2 [16]. By relying on static compression methods and differential thermal analysis, they reported a continuous reduction of the critical temperature for the $\alpha \rightarrow \beta$ transition (where β stands for the superionic phase) T_s under compression. This interesting and apparently puzzling effect has been overlooked for decades, calling for a meticulous revision with presently improved experimental techniques. Under a pressure of ∼10 GPa CaF_2 transforms into the orthorhombic cotunnite phase (γ, space group $Pnma$), which can be structurally related to the cubic α-phase through a local melting of the F^- sublattice [17]. The detailed ionic processes sustaining superionicity in this high-P γ phase, however, are totally uncertain [18]. As for theory, only a few simulation works have recently addressed the description of ionic conductivity at nonambient conditions [19,20]. Those few computational studies, however, all rely on molecular dynamics simulations performed with semiempirical pairwise potentials that have been tuned to reproduce the behavior of CaF_2 at ambient pressure. Whether the conclusions attained with those models at high $P-T$ conditions may still be regarded as reliable is an issue that needs clarification.

In this Letter, we present a combined experimental and first-principles computational study of the superionic and structural properties of CaF_2 at high P and high T. Our observations and simulations disclose an anomalous superionic behavior in α-CaF_2, which consists of a decrease of T_s in the pressure interval $5 \leq P \leq 8$ GPa. We find that such an anomaly can be caused by a P-induced softening of a zone-boundary X phonon, neither observed in SrF_2 nor in BaF_2. Regarding γ-CaF_2, our first-principles simulations show that large ionic conductivity is missing in this phase. Rather, superionicity develops once the crystal is transformed via a second-order transition into a new low-symmetry high-T phase that we identify as monoclinic (space group $P2_1/c$).

We carried out two sets of experiments in CaF_2 [water free, 99.9% purity (Sigma-Aldrich)] using a diamond-anvil cell (DAC). In the first set, Raman measurements were performed to determine the $\alpha-\gamma$ phase boundary [21]. In these experiments, a 514.5 nm Ar^+ laser was used for Raman excitation and silicone oil was chosen as the

pressure transmitting medium. The temperature was fixed using an electric heating sleeve that surrounds the DAC body, and was measured using a K-type thermocouple [22]. The R_1 photoluminescence line of ruby and the $^7D_0$-$^5F_0$ fluorescence of $SrB_4O_7:Sm^{2+}$ were used to determine P [23]. In the second set of experiments, CaF_2 acted as the pressure medium and it was heated using the laser-heating technique. A tungsten (W) foil embedded in the CaF_2 was heated with a Nd:YLF laser. The sample neither absorbs the laser radiation nor emits incandescent light in detectable amounts throughout all the studied P range. Therefore, following previous studies on alkali halides [24], T was measured from the W surface. Structural changes and melting were detected by visual observation using the laser speckle technique and a 632.8 nm He-Ne laser [25,26]. Temperatures were determined by fitting a Planck function to the thermal emission spectra of W. A series of at least four experiments was performed for each transition. The assigned transition temperature was the average of all the measurements, and the corresponding error was the maximum absolute deviation. After each heating cycle the DAC was inspected to check that neither chemical nor oxidation reactions had occurred in the metal surfaces [27]. The highest conditions reached in our experiments were $T \sim 25$ GPa and $P \sim 2500$ K.

Our first-principles density functional theory (DFT) calculations were performed with the generalized gradient approximation to the exchange-correlation energy [28]. We used the projector augmented wave method to represent the ionic cores, and considered Ca's $6p$-$2s$ and F's $2s$-$5p$ electronic states as valence. Wave functions were represented in a plane-wave basis truncated at 500 eV. By using these parameters and dense $\mathbf{k}$-point grids for the Brillouin zone integrations, we obtained enthalpies converged to within 3 meV per formula unit. In the geometry relaxations, we imposed a force tolerance of 0.01 eV Å^{-1}. The agreement between our zero-temperature DFT calculations and the experimental equation of state and Raman frequencies is fairly good (see Ref. [29]). Details of our one-phase and two-phase coexistence *ab initio* molecular dynamics (AIMD) simulations are explained in the Supplemental Material [29].

In Fig. 1, we show the results of our DAC measurements and first-principles simulations. As can be appreciated, the agreement between the experiments and calculations is remarkably good. Our results are also in accordance with previous data obtained by others at zero pressure [$T_s = 1400(90)$ K and the melting temperature $T_m = 1660(50)$ K] [8–12]. We attempted to estimate the $\alpha - \gamma$ boundary by performing DFT free energy calculations within the quasiharmonic approximation; however, as we will explain later, this approach turns out to be inadequate for CaF_2. The proposed CaF_2 phase diagram is very rich and complex: five different crystal phases [two of which are superionic (β and ϵ) and two are unknown

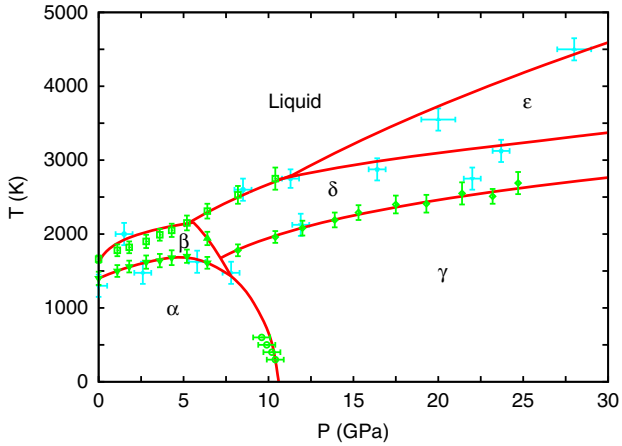

FIG. 1 (color online). Proposed phase diagram of CaF_2. Greek letters represent normal (α, γ, and δ) and superionic (β and ϵ) crystal phases, and the solid (red) lines their boundaries. Measurements and simulation results are indicated with open (green) and solid (blue) symbols, respectively.

(δ and ϵ)] and four special threefold coexistence points appear on it. Next, we concentrate on explaining the two findings that we deem as the most relevant: namely, (i) the observation of anomalous superionic behavior in α-CaF_2, and (ii) the appearance of two new phases at high T (δ and ϵ), one of which exhibits large ionic conductivity.

Anomalous superionic behavior in α-CaF_2.—Slow motion of the speckle pattern under steady laser illumination was ascribed to the $\alpha \rightarrow \beta$ transition (where β stands for the superionic state) in our experiments. A continuous and fast speckle motion observed at high temperatures, which was drastically different from the speckle motion observed in the $\alpha \rightarrow \beta$ transition, was assigned to melting. At $P = 6.4$ GPa, we observed changes in the laser-speckle pattern at three different temperatures. After our calculations, those changes were assigned to the $\alpha \rightarrow \beta$ transition [1610(80) K], to the $\beta \rightarrow \delta$ transition [1940(90) K], and to melting [2310(100) K]. The measured $\alpha - \beta$ boundary displays a positive variation with increasing pressure at low P, reaching a maximum of $T_s = 1700(90)$ at 5.2 GPa (in stark contrast to the data reported by Mirwald and Kennedy [16]). At larger compressions, however, dT_s/dP unexpectedly becomes negative (see Fig. 1). This is in fact a very intriguing effect: if superionicity was uniquely mediated by FPD, T_s should have necessarily increased upon raising P because the formation energy of FPD escalates with compression (as we show in the Supplemental Material [29]). Indeed, other arguments apart from FPD are needed to satisfactorily explain the observed T_s anomaly (and probably also superionicity).

In our AIMD simulations, we identified ionic conductivity by inspecting the calculated mean squared displacement $\Delta r^2(t)$ of the Ca^{+2} and F^- ions [20]. To ascertain that the crystal remained vibrationally stable (i.e., the thermal average position of each ion remains centered on its

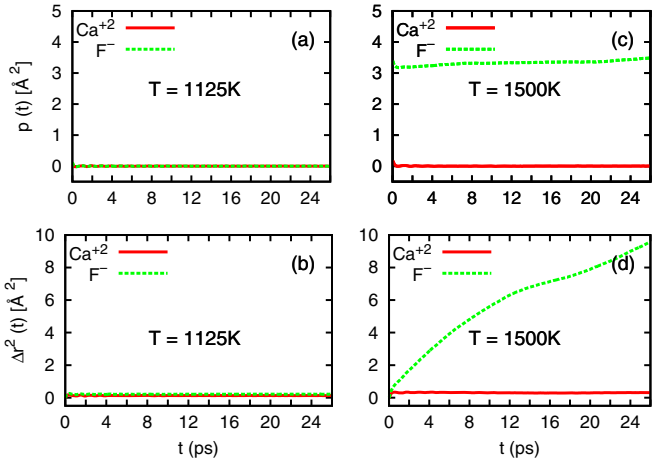

FIG. 2 (color online). Calculated position correlation function and mean squared displacement in CaF_2 at $T = 1125$ K (a),(b) and 1500 K (c),(d). $P \sim 0$ GPa. At 1500 (1125) K the system is in the β (α) phase (see text).

perfect-lattice site), we computed the position correlation function $p(t) \equiv \langle [\mathbf{r_i}(t + t_0) - \mathbf{R_i}^0] \cdot [\mathbf{r_i}(t_0) - \mathbf{R_i}^0] \rangle$, where $\mathbf{r_i}(t)$ is the position of ion i at time t, $\mathbf{R_i}^0$ its perfect-lattice position, t_0 is an arbitrary time origin, and $\langle \cdot \rangle$ denotes thermal average [see Figs. 2(a)–2(c)] [47,48]. The crystal is vibrationally stable if $p(t \to \infty) = 0$ since the displacements at widely separated times become uncorrelated. On the contrary, if the atoms acquire a permanent vibrational displacement, $p(t \to \infty)$ becomes nonzero. As shown in Fig. 1, the results obtained in our α-CaF_2 simulations are in very good agreement with our DAC measurements: a negative dT_s/dP slope is found at pressures higher than ~5 GPa. This remarkable agreement between theory and the experiments certifies that the reported P-induced T_s anomaly constitutes a genuine effect. We note that the classical simulation works performed to date have not reported any such peculiar behavior [19,20]; thus, we may conclude that current pairwise interaction models are unsuitable to emulate CaF_2 at high $P - T$ conditions.

In the search to rationalize the origins of the observed T_s anomaly, we turned our attention to collective phonon excitations [13–15]. Recently, an irregular T dependence of a low-energy phonon mode at the X point of the Brillouin-zone boundary (single degenerate, labeled here as X_2) has been observed in inelastic neutron scattering experiments [15]. That irregularity consists of a large decrease of its frequency with increasing temperature, which might be related to the onset of superionicity [13,14,49]. Motivated by these findings we studied the P dependence of this and another zone-boundary X mode (doubly degenerate, labeled here as X_1), both of which involve only the motion of F^- ions, with computational DFT methods (see Fig. 3) [29]. Our results show that the X_1 frequency is always the highest and that it increases mildly with compression. The X_2 mode, by contrast, softens significantly with pressure and its frequency eventually becomes imaginary at

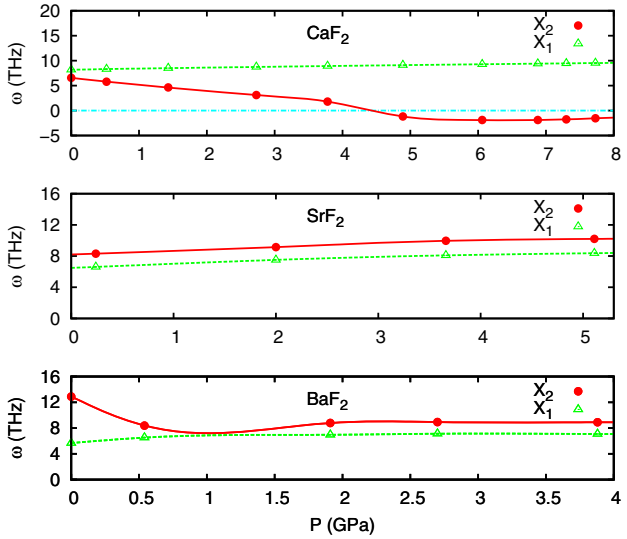

FIG. 3 (color online). Calculated frequencies of zone-boundary X phonon modes involving F^- displacements only, expressed as a function of pressure and AF_2 species (cubic α phase).

$P \sim 4.5$ GPa. This predicted phonon mode softening marks the appearance of a collective instability within the F^- sublattice at a pressure that is similar to that identified with the T_s anomaly. In particular, the X_2 eigenmode involves rows of anions moving antiphase along an edge of their cubic lattice; thus, it enhances F^- disorder [13,49]. We therefore link the causes behind the observed T_s anomaly with the predicted P-induced X_2 mode softening. The results enclosed in Fig. 3 also show that standard quasiharmonic approaches are inadequate to describe CaF_2 under pressure because of the presence of imaginary phonon frequencies, which are associated with large anharmonicity. Furthermore, aimed at disclosing whether the T_s anomaly could be observed also in other AF_2 compounds, we carried out analogous phonon calculations in α-SrF_2 and α-BaF_2 (see Fig. 3). Our results show that both X_1 and X_2 zone-boundary modes behave normally in these materials; thus, CaF_2 appears to be unique of its kind.

New high-T δ and superionic ϵ phases.—As γ-CaF_2 was stabilized in our DAC experiments and T increased steadily, we eventually observed a spatial fluctuation of the laser speckle that was markedly different from those found in the previous analyzed transitions: $\alpha \to \beta$ and melting. Specifically, an intermittent laser speckle motion was detected that could be interpreted as a recrystallization process. In order to shed light on the nature of these observations, we performed new exhaustive AIMD simulations on γ-CaF_2. The analysis of our computational results actually shows that the explained detections mark the occurrence of a continuous solid-solid transition (i.e., boundary $\gamma - \delta$ in Fig. 1).

In Figs. 4(a)–4(b), we enclose the Δr^2 and p functions obtained in CaF_2 at $P \sim 17$ GPa and $T = 2500$ K. The perfect-lattice positions entering the function p are those

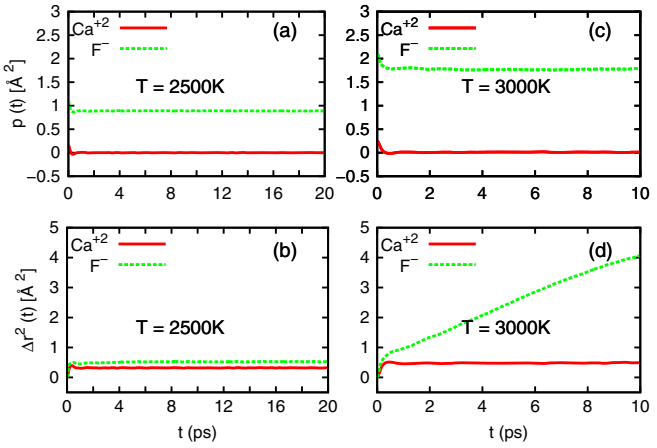

FIG. 4 (color online). Calculated position correlation function and mean squared displacement in CaF_2 at $T = 2500$ K (a),(b) and 3000 K (c),(d). $P \sim 17$ GPa. At 3000 (2500) K the system is in the ϵ (δ) phase [see text].

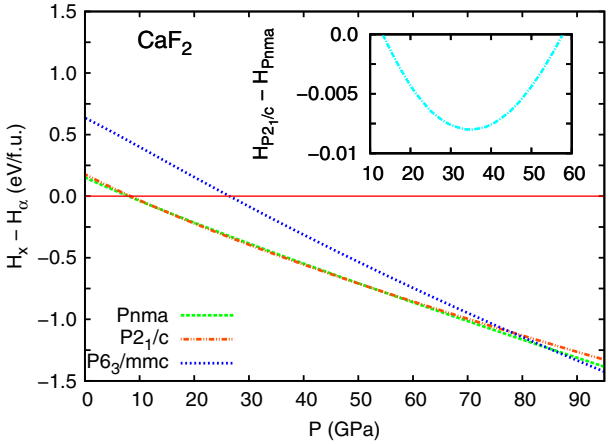

FIG. 5 (color online). Calculated enthalpy of several crystal structures referred to that of the cubic α phase and expressed as a function of pressure. Inset: detail of the enthalpy difference between the $P2_1/c$ and $Pnma$ phases.

of the cotunnite γ phase determined at zero temperature. The results in the figure reveal that at those conditions the diffusion of the F^- anions is null while the cotunnite γ phase becomes vibrationally unstable [that is, $\Delta r^2(t \to \infty) \sim$ const and $p(t \to \infty) \neq 0$ for the F^- anions]. In particular, the permanent displacements acquired by the fluorine anions suggest the occurrence of a continuous transformation from the cotunnite γ phase to a new unknown structure that we label as δ. We repeated our simulations at different $P - T$ conditions and always arrived at the same conclusions. Overall, our DFT estimations are in very good agreement with the series of measurements conforming the $\gamma - \delta$ boundary (see Fig. 1). By further raising T in our AIMD simulations, we found that large ionic conductivity appeared in the new high-T δ phase [see Figs. 4(c)–4(d)]. This constitutes a very important finding since up to now it has been assumed that under pressure superionicity appeared in the usual cotunnite γ phase [18]. We repeated our simulations at different $P - T$ conditions and determined the entire $\delta - \epsilon$ boundary, where ϵ stands for the new high-T superionic phase, up to ~25 GPa (see Fig. 1). Meanwhile, similar behavior to that just explained has not been reported in any previous classical simulation work; thus, we reaffirm our conclusion that currently available CaF_2 interaction models seem not to be adequate for high $P - T$ analysis.

In our search to identify the symmetry of the newly discovered δ phase, we initially turned our attention to the hexagonal $P6_3/mmc$ phase. Dorfman *et al.* recently reported a T-induced cotunnite to hexagonal phase transition in CaF_2 at pressures higher than ~60 GPa [50] (see Fig. 5); hence, the $P6_3/mmc$ phase seems to be a natural candidate. However, after running AIMD simulations we discarded this phase because the temperatures at which superionicity appeared were below the $\delta - \epsilon$ boundary. Subsequently, we carried out intensive crystal structure searches in compressed CaF_2 by relying on diverse strategies, all which are detailed in the Supplemental Material [29]. We found several structures that are energetically competitive with the γ phase at zero temperature: namely, $P2_12_12_1$, $Pmn2_1$, Pc, $P2_1$, and $P2_1/c$. Of these candidates, we first chose the orthorhombic $P2_12_12_1$ and $Pmn2_1$, and the monoclinic $P2_1/c$, phases because a group-subgroup relationship exists between them and the orthorhombic γ phase (a condition that is required for a continuous phase transition [51]). Finally, we concentrated on the monoclinic $P2_1/c$ phase because this one has the lowest energy. In Fig. 5, we plot the calculated enthalpy of this monoclinic phase in the $0 \leq P \leq 100$ GPa interval and show that it strongly rivals that of the cotunnite structure (actually, at some points both enthalpy curves are indistinguishable within the numerical errors). We also computed its phonon spectrum at several pressures and found that it is mechanically stable (see the Supplemental Material [29]). As a conclusive test, we performed new exhaustive AIMD simulations on the $P2_1/c$ phase and found that the calculated superionic temperatures were consistent with the $\delta - \epsilon$ boundary determined previously. Based on these outcomes, we identify the new high-T δ phase as monoclinic $P2_1/c$. This structure has a similar cation coordination polyhedra to that of the cotunnite phase: each Ca is linked to nine fluorine atoms that form an elongated tricapped trigonal prism [29]. Furthermore, we performed analogous enthalpy calculations in SrF_2 and BaF_2 under pressure and found that the monoclinic $P2_1/c$ phase is likewise energetically competitive in these materials (see the Supplemental Material [29]). Therefore, we may conclude that the $\gamma \to \delta$ and $\delta \to \epsilon$ transitions observed in CaF_2 are likely to occur also in SrF_2 and BaF_2.

In summary, based on combined experimental DAC and first-principles simulation investigations we have characterized the superionic conductivity in archetypal CaF_2 at high $P - T$ conditions, and elucidated further the physical

causes underlying it. The reliability of the reported results is supported by the concurrence of theory and experiment. Our findings are relevant also to a number of compounds that are isomorphic to CaF_2 including halides ($PbCl_2$), hydrides (CeH_2), nitrides (UN_2), and simple oxides (UO_2). We hope our results will stimulate future studies (e.g., using x-ray diffraction techniques) in the characterization of the β, δ, and ϵ phases of CaF_2.

This work was supported under the Australian Research Council's Future Fellowship funding scheme (Project No. RG134363), by Ministerio de Ciencia e Innovacion (Spain) (Grants No. MAT2010-18113, No. CSD2007-00041, No. MAT2013-46649-C4-1-P, No. CSD2007-00045, and No. FIS2008-03845), and by Generalitat Valenciana (Grant No. ACOMP/2014/243). Computer resources, technical expertise, and assistance were kindly provided by RES and CESGA. We acknowledge helpful comments from two of the referees on the proposed CaF_2 phase diagram.

*Corresponding author.

[1] J. Barth, R. L. Johnson, M. Cardona, D. Fuchs, and A. M. Bradshaw, Phys. Rev. B **41**, 3291 (1990).
[2] F. Gan, Y. N. Xu, M. Z. Huang, W. Y. Ching, and J. G. Harrison, Phys. Rev. B **45**, 8248 (1992).
[3] W. Hayes and A. M. Stoneham, *Defects and Defect Processes in Nonmetallic Solids* (Wiley, New York, 1985).
[4] M. J. Gillan, J. Phys. C **19**, 3391 (1986); J. Chem. Soc., Faraday Trans. **86**, 1177 (1990).
[5] P. J. D. Lindan and M. J. Gillan, J. Phys. Condens. Matter **5**, 1019 (1993).
[6] N. Sata, K. Eberman, K. Eberi, and J. Maier, Nature (London) **408**, 946 (2000).
[7] C. S. Cucinotta, G. Miceli, P. Raiteri, M. Krack, T. D. Kühne, M. Bernasconi, and M. Parrinello, Phys. Rev. Lett. **103**, 125901 (2009).
[8] C. E. Derrington, A. Lindner, and M. O'Keeffe, J. Solid State Chem. **15**, 171 (1975).
[9] W. Hayes and M. T. Hutchings in *Ionic Solids at High Temperatures* (World Scientific, Singapore, 1985).
[10] G. A. Evangelakis and V. Pontikis, Europhys. Lett. **8**, 599 (1989).
[11] S. D. Mclaughlan, Phys. Rev. **160**, 287 (1967).
[12] A. Mitchell and S. Joshi, Metall. Trans. **3**, 2306 (1972).
[13] L. L. Boyer, Phys. Rev. Lett. **45**, 1858 (1980).
[14] L. X. Zhou, J. R. Hardy, and H. Z. Cao, Solid State Commun. **98**, 341 (1996).
[15] K. Schmalzl, D. Strauch, and H. Schober, Phys. Rev. B **68**, 144301 (2003).
[16] P. W. Mirwald and G. C. Kennedy, J. Phys. Chem. Solids **39**, 859 (1978).
[17] S. E. Boulfelfel, D. Zahn, O. Hochrein, Y. Grin, and S. Leoni, Phys. Rev. B **74**, 094106 (2006).
[18] S. Hull and D. A. Keen, Phys. Rev. B **58**, 14837 (1998).
[19] Z.-Y. Zeng, X.-R. C hen, J. Zhu, and C.-E Hu, Chin. Phys. Lett. **25**, 230 (2008).
[20] C. Cazorla and D. Errandonea, J. Phys. Chem. C **117**, 11292 (2013).
[21] S. Speziale and T. S. Duffy, Phys. Chem. Miner. **29**, 465 (2002).
[22] D. Errandonea, D. Martínez-García, A. Segura, A. Chevy, G. Tobias, E. Canadell, and P. Ordejón, Phys. Rev. B **73**, 235202 (2006).
[23] F. Datchi, R. Le Toulec, and P. Loubeyre, J. Appl. Phys. **81**, 3333 (1997).
[24] R. Boehler, M. Ross, and D. B. Boercker, Phys. Rev. B **53**, 556 (1996).
[25] D. Errandonea, R. Boehler, and M. Ross, Phys. Rev. Lett. **85**, 3444 (2000).
[26] D. Errandonea, Phys. Rev. B **87**, 054108 (2013).
[27] D. Errandonea, J. Phys. Chem. Solids **70**, 1117 (2009).
[28] J. P. Perdew, K. Burke, and M. Ernzerhof, Phys. Rev. Lett. **77**, 3865 (1996).
[29] See Supplemental Material at http://link.aps.org/supplemental/10.1103/PhysRevLett.113.235902, which includes Refs. [30–46], for details of the DFT calculations, formation energy of FPD, X_2 phonon mode, crystal structure searches, and monoclinic $P2_1/c$ phase.
[30] A. Kavner, Phys. Rev. B **77**, 224102 (2008).
[31] L. Gerward, J. S. Olsen, S. Steenstrup, M. Malinowski, S. Asbrink, and A. Waskowska, J. Appl. Crystallogr. **25**, 578 (1992).
[32] G. Kresse, J. Fürthmuller, and J. Hafner, Europhys. Lett. **32**, 729 (1995).
[33] D. Alfè, G. D. Price, and M. J. Gillan, Phys. Rev. B **64**, 045123 (2001).
[34] D. Alfè, Comput. Phys. Commun. **180**, 2622 (2009).
[35] X. Gonze and J.-P. Vigneron, Phys. Rev. B **39**, 13120 (1989).
[36] S. Baroni, S. de Gironcoroli, A. del Corso, and P. Giannozzi, Rev. Mod. Phys. **73**, 515 (2001).
[37] Y. Wang, J. J. Wang, W. Y. Wang, Z. G. Mei, S. L. Shang, L. Q. Chen, and Z. K. Liu, J. Phys. Condens. Matter **22**, 202201 (2010).
[38] C. Cazorla and J. Íñiguez, Phys. Rev. B **88**, 214430 (2013).
[39] C. Cazorla, M. J. Gillan, S. Taioli, and D. Alfè, J. Chem. Phys. **126**, 194502 (2007).
[40] S. Taioli, C. Cazorla, M. J. Gillan, and D. Alfè, Phys. Rev. B **75**, 214103 (2007).
[41] C. Cazorla, D. Alfè, and M. J. Gillan, J. Chem. Phys. **130**, 174707 (2009).
[42] D. Alfè, C. Cazorla, and M. J. Gillan, J. Chem. Phys. **135**, 024102 (2011).
[43] D. Alfè, Phys. Rev. B **79**, 060101(R) (2009).
[44] H. T. Stokes, D. M. Hatch, and B. J. Campbell, ISOTROPY, http://stokes.byu.edu/isotropy.html.
[45] B. K. Godwal, S. Speziale, M. Voltolini, R. Wenk, and R. Jeanloz, Phys. Rev. B **82**, 064112 (2010).
[46] B. K. Godwal, S. Stackhouse, J. Yan, S. Speziale, B. Militzer, and R. Jeanloz, Phys. Rev. B **87**, 100101(R) (2013).
[47] C. Cazorla, D. Alfè, and M. J. Gillan, Phys. Rev. B **85**, 064113 (2012).
[48] L. Vočadlo, D. Alfè, M. J. Gillan, I. G. Wood, J. P. Brodholt, and G. D. Price, Nature (London) **424**, 536 (2003).
[49] L. L. Boyer, Solid State Ionics **5**, 581 (1981).
[50] S. M. Dorfman, F. Jiang, Z. Mao, A. Kubo, Y. Meng, V. B. Prakapenka, and T. S. Duffy, Phys. Rev. B **81**, 174121 (2010).
[51] H. T. Stokes and D. M. Hatch, Phys. Rev. B **30**, 4962 (1984).